Video Article

Advanced Compositional Analysis of Nanoparticle-polymer Composites Using Direct Fluorescence Imaging

Colin R. Crick*[1], Sacha Noimark*[2,3], William J. Peveler*[3], Joseph C. Bear[3], Aleksandar P. Ivanov[1], Joshua B. Edel[1], Ivan P. Parkin[3]

[1]Department of Chemistry, Imperial College London

[2]Department of Medical Physics and Biomedical Engineering, University College London

[3]Department of Chemistry, University College London

*These authors contributed equally

Correspondence to: Colin R. Crick at c.crick@imperial.ac.uk

URL: http://www.jove.com/video/54178
DOI: doi:10.3791/54178

Keywords: Engineering, Issue 113, Nanoparticle, Swell Encapsulation, Nanocomposite, Quantum dots, Polydimethylsiloxane, Fluorescent, Fluorescence Imaging, Functional Material, Physics

Date Published: 7/19/2016

Citation: Crick, C.R., Noimark, S., Peveler, W.J., Bear, J.C., Ivanov, A.P., Edel, J.B., Parkin, I.P. Advanced Compositional Analysis of Nanoparticle-polymer Composites Using Direct Fluorescence Imaging. *J. Vis. Exp.* (113), e54178, doi:10.3791/54178 (2016).

Abstract

The fabrication of polymer-nanoparticle composites is extremely important in the development of many functional materials. Identifying the precise composition of these materials is essential, especially in the design of surface catalysts, where the surface concentration of the active component determines the activity of the material. Antimicrobial materials which utilize nanoparticles are a particular focus of this technology. Recently swell encapsulation has emerged as a technique for inserting antimicrobial nanoparticles into a host polymer matrix. Swell encapsulation provides the advantage of localizing the incorporation to the external surfaces of materials, which act as the active sites of these materials. However, quantification of this nanoparticle uptake is challenging. Previous studies explore the link between antimicrobial activity and surface concentration of the active component, but this is not directly visualized. Here we show a reliable method to monitor the incorporation of nanoparticles into a polymer host matrix *via* swell encapsulation. We show that the surface concentration of CdSe/ZnS nanoparticles can be accurately visualized through cross-sectional fluorescence imaging. Using this method, we can quantify the uptake of nanoparticles *via* swell encapsulation and measure the surface concentration of encapsulated particles, which is key in optimizing the activity of functional materials.

Video Link

The video component of this article can be found at http://www.jove.com/video/54178/

Introduction

The application of nanomaterials has long served as an area of increasing interest for novel technologies.[1-3] This has included the growing use of nanoparticles in everyday items, including cosmetics, clothes, packaging and electronics.[4-6] A major drive toward using nanoparticles in functional materials stems from their higher reactivity relative to the materials, in addition to the ability to tune properties by variation in particle size.[7] One further advantage is the capability to easily form composite materials, introducing crucial properties to the host matrix, such as catalytic functionality, material strengthening and tuning of electrical properties.[8-12]

Nanoparticle-polymer composite materials can be achieved through a range of techniques, the simplest of which is direct integration of the desired nanoparticles during the fabrication of the host matrix.[13,14] This results in a homogenous material with an even spacing of nanoparticulate material throughout. However, many applications only require the active material to be present at the external interfaces of the nanocomposites. As a result, direct incorporation does not result in efficient use of sometimes costly nanoparticle material as there is much nanoparticle waste through the bulk of the material.[15,16] To achieve direct incorporation, the nanoparticles must also be compatible with host matrix formation. This may be challenging, especially in syntheses that require multifaceted reactions such as in the case of thermosetting polymers that are typically facilitated by metal complex catalysts mechanisms that may be affected by highly active nanoparticles.[14]

The considerable disadvantages associated with direct nanoparticle incorporation during the polymer synthesis, has led to the development of techniques aimed to limit nanoparticle incorporation to the surface layer.[17-21] Swell encapsulation is one of the most successful strategies reported in the literature, to achieve high surface nanoparticle concentrations, with limited wastage in the polymer bulk.[17-19] The technique utilizes the solvent driven swelling of polymer matrices, allowing for the incursion of molecular species and nanoparticles. Upon removal of the swelling solvent, the species within the matrix become fixed into place, with the highest concentration of species localized at the surface. To date, most of the reported uses of swell encapsulation are directed toward the fabrication of antimicrobial polymers, where it is key that the active agents are at the material surface. While many of these reports show enhanced antimicrobial activity, the precise surface nanoparticle composition is rarely probed in detail. Crick *et al.* recently demonstrated a method for the direct visualization of nanoparticle incursion, providing crucial insight into the kinetics and surface nanoparticle concentrations achieved by swell encapsulation.[22]

This work details the synthesis of cadmium selenide quantum dots (QD), their swell encapsulation into polydimethylsiloxane (PDMS) and the direct visualization of their incorporation using fluorescence imaging. The effect of varying swell encapsulation time and nanoparticle concentration in the swelling solution is explored. The fluorescence visualization technique allows for the direct imaging of nanoparticle incursion into the PDMS and demonstrates that the highest concentration of QDs is at the material surface.

Protocol

1. Preparation of CdSe/ZnS Core/Shell Quantum Dots

1. **Preparation of the trioctylphosphine (TOP)-Se solution**
    1. Prepare a 0.5 M solution of selenium in TOP by mixing the appropriate amount of Se into TOP in a Schlenk flask under nitrogen or in a glovebox (8 ml required per reaction, typically 0.4 g dissolved in 10 ml of TOP).
    2. Stir the mixture to dissolve the Se for 1 hr, resulting in a grey solution of the TOP-Se complex.
    3. Ensure the solution is then freeze-pump-thaw degassed 5 times. The resulting stock solution can be stored under nitrogen for 3 months.

2. **Preparation of the CdSe Cores**
    1. Weigh out cadmium oxide (51 mg, 0.4 mmol), TOP oxide (3.7 g, 9.6 mmol), hexadecylamine (1.93 g, 8 mmol) and 1-dodecylphosphonic acid (0.22 g, 0.88 mmol) and combine into a three neck, 250 ml round bottom flask. Add a stir bar.
    2. Close two necks with septa and ensure the third is attached to a long reflux condenser and a nitrogen/vacuum Schlenk line. Insert a heating mantle temperature probe through one septum directly into the mixture. Pump/refill the flask with nitrogen five times.
    3. Heat the flask to 320 °C and stir the melt for 1 hr under a nitrogen atmosphere.
    4. Lower the temperature of the mantel to 270 °C and then use a large syringe and wide bore needle (20 ml, 3 mm bore) to degas with nitrogen 5 times.
    5. Take up 8 ml of the TOP-Se solution (step 1.1) and inject carefully but rapidly into the three neck flask, through the septum.
    6. Stir the reaction at 270 °C for between 30 sec and 10 min to control the size of particles produced. For red emission (~ 600 nm), 7-9 min is suitable.
    7. Prepare a bowl of boiling water (large enough to submerge half of the reaction vessel) and place next to the reaction mixture. After the reaction time is complete, rapidly cool the reaction in the boiling water with swirling.
    CAUTION: Cooling can cause the flask to crack. Take great care and wear thick impervious gloves.
    8. Once cool, inject 10 ml of chloroform into the flask to dissolve all the products, and divide the mixture between two 50 ml centrifuge tubes.
    9. Top up each tube up to 50 ml with EtOH and centrifuge at 3,600 × g for 10 min to precipitate the particles. Discard the supernatant and re-disperse the pellets in a total of 10 ml of n-hexane.

3. **ZnS Shelling of the CdSe Core:**
    1. Add the cores in hexane to a 100 ml round bottom flask containing zinc diethyldithiocarbamate (0.5 g, 1.4 mmol), oleylamine (3 ml, 9.12 mmol), trioctylphosphine (3 ml, 6.73 mmol) and 1-octadecene (10 ml). Add a stir bar. Exchange the reaction atmosphere to nitrogen.
    2. Heat the reaction on a hotplate-stirrer at 3.3 °C/min under partial vacuum until 70 °C, and remove the hexane using the Schlenk line.
    3. Switch the atmosphere to nitrogen and continue heating at this rate to 120 °C. Stir at 120 °C for 2 hr.
    4. Allow the reaction to cool, and split the mixture between 2 × 50 ml centrifuge tubes. Ensure the tubes are topped up to 50 ml with EtOH to precipitate the particles and centrifuge at 3,600 × g for 10 min.
    5. Discard the supernatant and re-disperse the pellets in a total of 10 ml of n-hexane.
    6. Centrifuge this solution (3,600 x g, 10 min) once more to remove any insoluble impurities, before being decanted into a sample tube, and store in the fridge (4 °C) under a nitrogen atmosphere for up to three months.

2. Swelling Encapsulation of Nanoparticles into PDMS

1. **Swelling Solution Preparation:**
    1. Prepare a stock solution of CdSe QDs by mixing 36 ml of n-hexane with 4 ml of CdSe QD dispersion (as synthesized) and stir the solution magnetically.
    2. Set aside two vials each containing 9 ml of the stock solution as designated swelling solutions.
    3. Use the remainder of the stock solution for the preparation of further swelling solutions of varying QD concentrations. Prepare three swelling solutions of decreasing QD concentration by diluting the stock solution to give a 66% (v/v) solution, 50% solution and 33% solution.
        1. Prepare the 66% (v/v) solution by mixing 6 ml of the CdSe QD stock solution with 3 ml n-hexane. Stir the solution magnetically to ensure complete mixing.
        2. Prepare the 50% (v/v) solution by mixing 4.5 ml of the CdSe QD stock solution with 4.5 ml n-hexane. Stir the solution magnetically to ensure complete mixing.
        3. Prepare the 33% (v/v) solution by mixing 3 ml of the CdSe QD stock solution with 6 ml n-hexane. Stir the solution magnetically to ensure complete mixing.
    4. Store all of the QD solutions under dark conditions, at room temperature.

2. **Polymer Preparation and QD Incorporation - Varying the QD Concentration in the Swelling Solution:**
    1. Cut out four medical grade silicone squares (11 mm x 11 mm) using a fresh scalpel blade.

2. Immerse a medical grade silicone square in each of the four swelling solutions of varying % QD concentration: stock solution, 66% (v/v), 50% (v/v) and 33% (v/v). Allow the polymer samples to swell for 24 hr under dark conditions, and at room temperature.
3. Remove the swollen polymer samples from the respective swelling solutions and air dry under dark conditions for 48 hr, during which time the residual solvent evaporates and the polymers shrink back to their initial dimensions.
4. Wash the QD-incorporated samples thoroughly with deionized water to remove any surface bound materials.

3. **Polymer Preparation and QD Incorporation - Varying the Polymer Exposure Time to the Swelling Solution:**
   1. Prepare four more medical grade silicone squares (11 mm x 11 mm), as noted in 2.2.1.
   2. Immerse the medical grade silicone squares in the stock swelling solution for varying time periods: 1 hr, 3 hr, 6 hr and 24 hr.
   3. After removal from the swelling solution, air dry the swollen polymer samples under dark conditions for 48 hr, such that the sample shrinks back to its previous dimensions.
   4. Wash the QD-incorporated samples thoroughly with deionized water to remove any surface bound materials or residual solvent.

3. Visualization of Nanoparticle Swell Encapsulation into PDMS

1. **Silicone Sample Preparation:**
   1. Cut out two silicone squares with a fresh scalpel blade (5.5 mm x 11 mm). Ensure that this exposes the internal surface of the silicone samples.

2. **Fluorescence Imaging:**
   1. Place the silicone samples on a microscope slide for imaging, ensuring that the freshly cut side of the polymer makes full contact with the glass slide. Press the silicone portion down lightly to ensure a smooth contact with the microscope slide. Place the sample on the stage of the microscope.
   2. Complete lifetime fluorescence measurements using a 488 nm spectrally filtered laser line comprising of 5 psec pulses at a rate of 20 MHz or similar.[23] Use an acousto-optic tunable filter system, to directly couple to the laser output, in order to generate the 488 nm laser line. Focus the laser beam using a custom-built laser-scanning unit (see supplementary information), which is reflected by a dichroic mirror (488 nm) into the back aperture of a 10X objective and then onto the sample.
      1. Collect the fluorescence emission with the same objective, that then passes through the same dichroic mirror. Direct this light towards an avalanche photodiode operating in single photon counting mode. Process lifetime measurements using a time-correlated single photon counting (TCSPC) board.[23]
   3. Record the instrument response function (IRF) at the beginning and the end of each experimental session.[23]
      Note: The recorded signal in the TCSPC experiment should show the time delay between the photons arrival at the detector and the production of the subsequent laser pulse. This time delay however, should be convolved with the IRF of the measuring apparatus. Hence, the IRF is measured as the response of the instrument to 100 nM Auramine O, which has a significantly shorter lifetime (~100 psec) compared to the instrumental response.
   4. Extract the lifetime by non-linear fitting of the exponential decay of the fluorescent intensity and deconvolute this from the IRF using a maximum likelihood estimator (MLE) algorithm[25-27]. The MLE (γ_j) is calculated as
      $$\gamma_j = \sum_{1}^{k} n_i \log\left(\frac{n_i}{N p_i(j)}\right)$$
      Where n_i is the number of photon counts in channel i, k is the number of channels (or bins) for each fluorescence decay, $p_i(j)$ is the probability that a group of photons will fall in channel *i* if the particles have a lifetime *j*, and *N* is the total number of counts for a given decay.
   5. Record each sample fluorescence intensity and lifetime data for 5 min, creating a continuous scan consisting of 264 images with size 512 × 512 pixels. Combine these to provide two-dimensional fluorescence intensity, lifetime and intensity weighted lifetime maps, with a calculated MLE with threshold of 150 photons and process this using MATLAB.

Representative Results

The quantum dots exhibited red fluorescence, with a lambda max of approximately 600 nm.[22,28] The red emission was due to the confinement of the exciton by the quantum rod whose size dimensions are within the strong confinement regime. Li *et al.* showed that for quantum rods, the emission shifts to lower energy with an increase in either width or length of the rod. They further showed that the emission mainly determined by the lateral confinement, which plays an important role even when rods are very long, especially when the width is less than the Bohr radius of the material in question as it is in the strong confinement regime.[29] Transmission electron microscope (TEM) imaging shows the elongated shape of the QDs (aspect ratio ~2.5). The average length of the QDs was shown to be 12.6 nm ± 2.1 nm (n = 200) (**Figure 1**). The QD solutions were stable under refrigeration for up to 3 months. Lower magnification images of the QDs are provided in the supplementary information (SI - 1).

During the encapsulation process, the silicone samples visually swelled, expanding to a maximum size of 15 mm × 15 mm × 2 mm after 1 hour in the swelling (original dimensions, 11 mm × 11 mm × 1 mm). The samples shrunk to their original size once the residual solvent evaporated (**Figure 2**). UV-Vis spectroscopy showed that nanoparticle encapsulation did not affect polymer coloration, whereby spectra remained unchanged for all of the encapsulated samples. Scanning electron microscope (SEM) imaging of the silicone subsequent to swell encapsulation showed that wrinkling at the surface, caused by the swell-shrink process. Energy dispersive X-ray spectroscopy (EDS) analysis showed evidence of the CdSe QDs, and indicated there was an increase in the presence of these elements (Cd/Se) with swelling time. The large detection volume of the EDS analysis did not allow for reliable quantitative analysis of surface coverage. SEM image and EDS data is provided in supplementary information (SI - 2/3).

The profile of the nanoparticle penetration through the polymer was shown through cross-sectional cutting of the silicone samples, in combination with laser excitation (microscope setup shown in supplementary information SI - 4). The fluorescent QD nanoparticles responded to the 488 nm incident laser scanning, emitting light in the red portion of the visible spectrum. The sample data indicated that CdSe QDs were concentrated at the external surfaces of the silicone, with a substantially reduced signal originating from the center of the sample. The incursion of the QDs into the silicone polymer was imaged using two-dimensional intensity weighted lifetime (τw) maps (photon count × lifetime). The exposure of the cross-sectional profile along the middle of silicone samples ensured that the full extent of nanoparticle movement through the polymer could be visualized (**Figure 3**). Longer swell encapsulation times (48 hours) provided samples with both the highest surface concentration of particles, and highest amount of particle permeation through to the bulk of the polymer, right through to the sample center. Shorter times encapsulation times (1, 4 and 24 hours) still show a higher number of particles at the surface, however the number of particles is reduced (**Figure 3**). Serial dilutions from the stock solution (100%) were used to investigate the effects of varying the nanoparticle concentration, on the subsequent uptake of nanoparticles into the polymer. The stock solution was diluted to achieve the following relative concentration swelling solutions to 66%, 50% and 33% v:v. No discernible differences in the fluorescence imaging was observed when the concentration was varied, when swell encapsulated for 48 hours, indicating that the swelling solution nanoparticle concentration does not impact the nanoparticle uptake into the polymer.

The highest nanoparticle surface concentration was observed for samples swell encapsulated for 48 hours. The fluorescence intensity of these samples is comparable to that in the swelling solution [~ 0.7 μM] (Supplementary information - SI - 5). The maximum penetration of particles is shown to be ~ 163 μm from the outer edge, with the concentration reaching half-maximum after 100 μm. The rate of maximum particle penetration is shown to slow as encapsulation time is increase, increasing from an average penetration rate of 3.4 μm/hour for 48 hours samples, to a rate of 28 μm/hour samples swell encapsulated for 4 hours (Supplementary information - SI - 5).

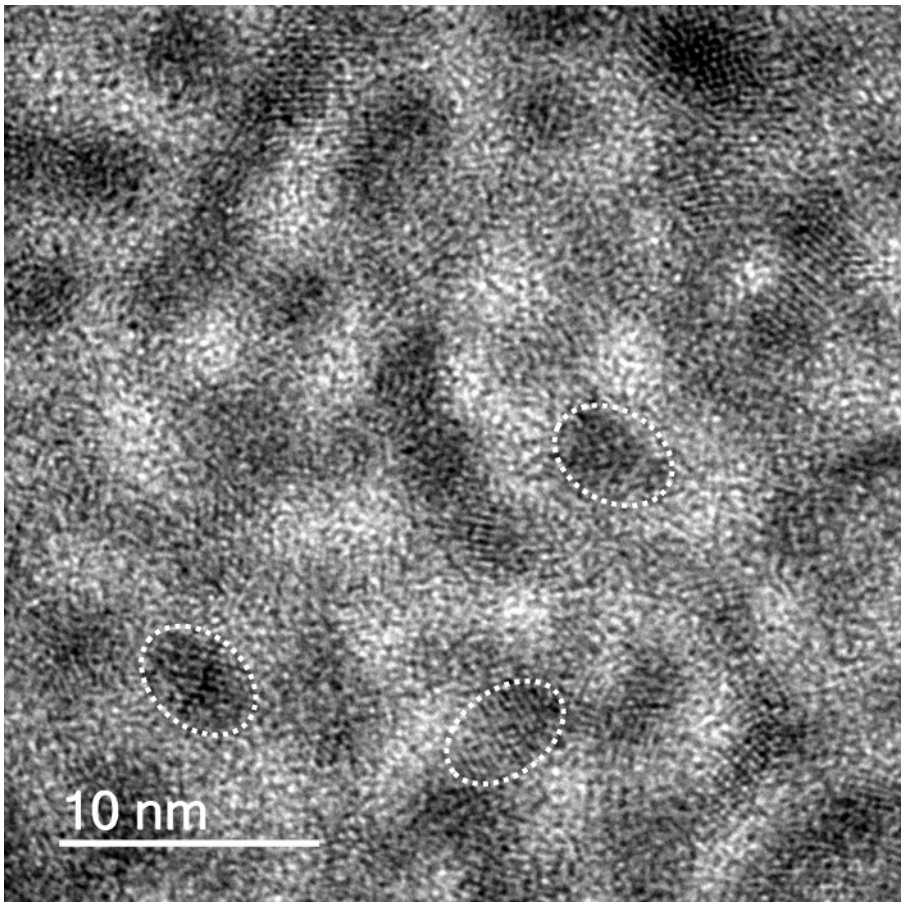

Figure 1. Quantum Dot Images. CdSe/ZnS QD TEM images showing rod like nanoparticles. Scale bar shows 10 nm. Outlines of individual particles are overlaid. Please click here to view a larger version of this figure.

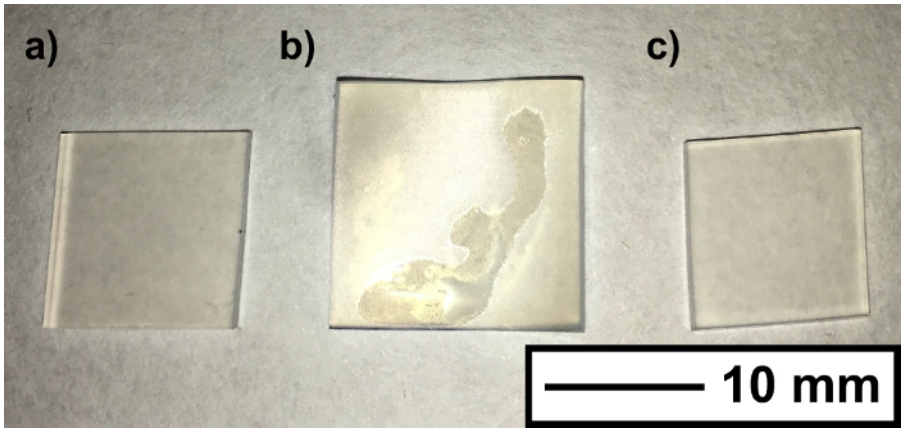

Figure 2. Polymer Swelling. Photograph shows the silicone samples (**a**) before, (**b**) during and (**c**) after the solvent induced swelling. The size increase (from 11 mm to 15 mm), is reversed upon full drying of the silicone. Scale bar shows 10 mm. Please click here to view a larger version of this figure.

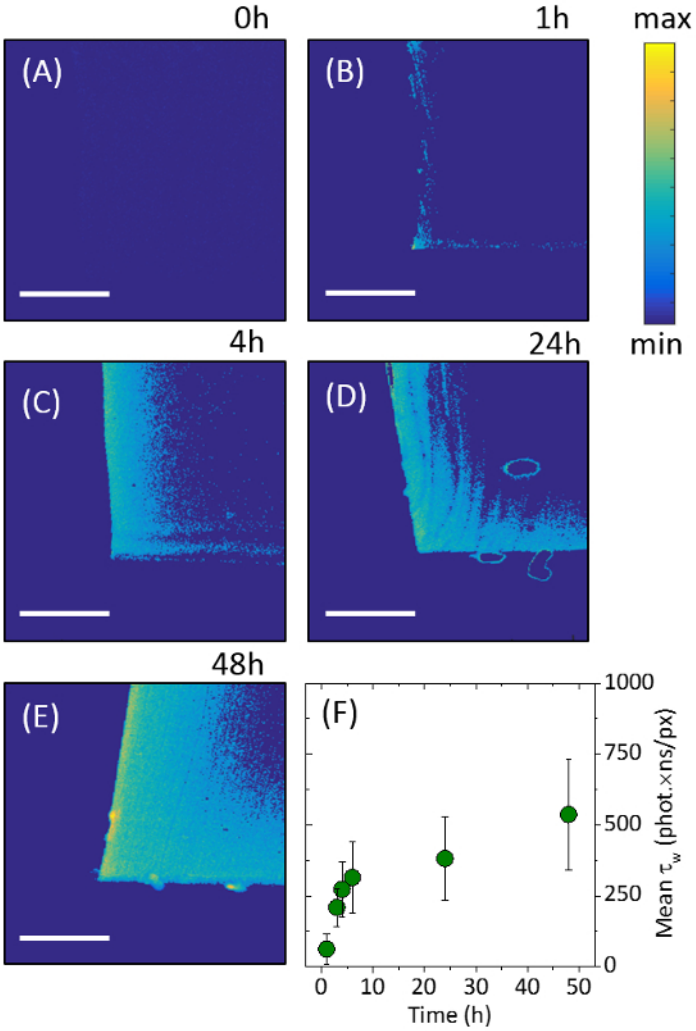

Figure 3. Fluorescence Lifetime Images. Images showing 2D intensity weighted lifetime maps (photon count lifetime). The images show the cross-sectional profiles of the center of the polymer portions after: (**A**) 0 hours, (**B**) 1 hour, (**C**) 4 hours, (**D**) 24 hours and (**E**) 48 hours of swell-encapsulation. (**F**) Encapsulation progress is shown by analyzing the normalized intensity weighed lifetime for each image. Scale bars show 100 µm. Error bars are show one standard deviation of the variation in the results obtained. This figure has been modified from [22], reproduced by permission of The Royal Society of Chemistry. Please click here to view a larger version of this figure.

Discussion

Cross-sectional fluorescence imaging allows for direct visualization of nanoparticles during swell encapsulation. The kinetics of encapsulation has been shown, with the drive toward a high nanoparticle surface concentration demonstrated. The extent of nanoparticle incorporation is shown to vary with swell encapsulation time (described in section 2.3), with the total amount of incorporated nanoparticles increasing as this time is extended, with the particle concentration localized at the surface if the polymer samples are used. The variation in the concentration of the nanoparticle solution (up to a 3× dilution, described in section 2.2), indicates there is little change in the amount of encapsulated particles. The swell encapsulation behavior of the particles used (CdSe QDs, Ø - 12.6 ± 2.1 nm) have also been shown to be comparable to particles of similar size (Titanium dioxide, Ø - 13.1 ± 5.6 nm),[22] which demonstrates the potential use of this technique as a valuable tool for further investigating swell encapsulation kinetics. The swell encapsulation rates observed in these experiments are imagined to be sensitive to nanoparticle size, and so any size variation may result in a modification of the encapsulation rate.

The accurate quantification of nanoparticles within nanocomposites is a challenge that faces many research groups.[1-3] Fundamental methods exist which allow the identification of a materials overall composition, however an substantial increase in complexity arises when assessing localized nanoparticle concentration, or concentration gradients over micrometer (or even nanometer) distances. Existing standards rely upon bulk measurements, such as EDS and XPS, in addition to estimating the surface concentration through functional testing, however using these methods means the precise surface composition would remain unknown.[17-21] The analysis technique detailed herein, provides direct imaging and facilitates quantitative analysis of these materials. Quantification of precise nanoparticle concentrations within the polymer is possible, when the fluorescence images are evaluated against known concentrations of the fluorescent material. It is hoped that the techniques described are able to contribute toward a developing a standard test for accurate surface concentration analysis of nanocomposites to further research in the development of more potent antimicrobial materials, as well as functional materials.

Cross-sectional fluorescence imaging has the potential to be applied to any fluorescent nanoparticulate species, it is possible that the fluorescence could originate from the nanoparticle itself or the surrounding ligands. Limitations of this technique will stem from the inability to incorporate nanoparticulate fluorescent species. Future developments of these experiments could aim to explore the nanoparticle size dependence of the swell encapsulation rate, with the composition of the swelling solvent also a potential focus. The development of a full understanding of the encapsulation process will be vital in the advance of swell encapsulation as a process for fabricating functional materials.

Disclosures

The authors have nothing to disclose.

Acknowledgements

C.R.C. would like to acknowledge the Ramsay Memorial Trust for funding.

References

1. Pumera, M. Graphene-based nanomaterials and their electrochemistry. *Chem. Soc. Rev.* **39** (11), 4146-4157 (2010).
2. Zhang, Q., Uchaker, E., Candelaria, S. L., & Cao, G. Nanomaterials for energy conversion and storage. *Chem. Soc. Rev.* **42** (7), 3127-3171 (2013).
3. Tong, H., Ouyang, S., Bi, Y., Umezawa, N., Oshikiri, M., & Ye, J. Nano-photocatalytic Materials: Possibilities and Challenges. *Adv. Mater.* **24** (2), 229-251 (2012).
4. Olson, M. S., & Gurian, P. L. Risk assessment strategies as nanomaterials transition into commercial applications. *J. Nanopart. Res.* **14** (4), 1-7 (2012).
5. Noimark, S., Dunnill, C. W., & Parkin, I. P. Shining light on materials - A self-sterilising revolution. *Adv. Drug Deliv. Rev.* **65** (4), 570-580 (2013).
6. Lavik, E., & von Recum, H. The Role of Nanomaterials in Translational Medicine. *ACS Nano.* **5** (5), 3419-3424 (2011).
7. Meier, J., Schiøtz, J., Liu, P., Nørskov, J. K., & Stimming, U. Nano-scale effects in electrochemistry. *Chem. Phys. Lett.* **390** (4-6), 440-444 (2004).
8. Booß-Bavnbek, B., Klösgen, B., Larsen, J., Pociot, F., & Renström, E. *BetaSys: Systems Biology of Regulated Exocytosis in Pancreatic ß-Cells. Springer Science & Business Media* (2011).
9. Xu, Z. P., Zeng, Q. H., Lu, G. Q., & Yu, A. B. Inorganic nanoparticles as carriers for efficient cellular delivery. *Chem. Eng. Sci.* **61** (3), 1027-1040 (2006).
10. Ito, A., Shinkai, M., Honda, H., & Kobayashi, T. Medical application of functionalized magnetic nanoparticles. *J. Biosci. Bioeng.* **100** (1), 1-11 (2005).
11. Xiu, F.-R., & Zhang, F.-S. Size-controlled preparation of Cu2O nanoparticles from waste printed circuit boards by supercritical water combined with electrokinetic process. *J Hazard. Mater.* **233-234**, 200-206 (2012).
12. Ponja, S., *et al.* Aerosol assisted chemical vapour deposition of hydrophobic TiO2-SnO2 composite film with novel microstructure and enhanced photocatalytic activity. *J. Mater. Chem., A* **1** (20), 6271-6278 (2013).
13. Crick, C. R., Bear, J. C., Kafizas, A., & Parkin, I. P. Superhydrophobic Photocatalytic Surfaces through Direct Incorporation of Titania Nanoparticles into a Polymer Matrix by Aerosol Assisted Chemical Vapor Deposition. *Adv. Mater.* **24** (26), 3505-3508 (2012).
14. Crick, C. R., Bear, J. C., Southern, P., & Parkin, I. P. A general method for the incorporation of nanoparticles into superhydrophobic films by aerosol assisted chemical vapour deposition. *J. Mater. Chem., A.* **1** (13), 4336-4344 (2013).

15. Jensen, G. C., Krause, C. E., Sotzing, G. A., & Rusling, J. F. Inkjet-printed gold nanoparticle electrochemical arrays on plastic. Application to immunodetection of a cancer biomarker protein. *Phys. Chem. Chem. Phys.* **13** (11), 4888-4894 (2011).
16. Steigerwald, A., & Mu, R. Potential of pulsed electron-beam deposition for nanomaterial fabrication: Spatial distribution of deposited materials. *J. Vac. Sci. Technol., B.* **26** (3), 1001-1005 (2008).
17. Perni, S., *et al.* Antibacterial Activity of Light-Activated Silicone Containing Methylene Blue and Gold Nanoparticles of Different Sizes. *J. Cluster Sci.* **21** (3), 427-438 (2010).
18. Perni, S., *et al.* The antimicrobial properties of light-activated polymers containing methylene blue and gold nanoparticles. *Biomater.* **30** (1), 89-93 (2009).
19. Noimark, S., *et al.* Dual-Mechanism Antimicrobial Polymer-ZnO Nanoparticle and Crystal Violet-Encapsulated Silicone. *Adv. Func. Mater.* **25** (9), 1367-1373 (2015).
20. Gingery, D., & Bühlmann, P. Formation of gold nanoparticles on multiwalled carbon nanotubes by thermal evaporation. *Carbon.* **46** (14), 1966-1972 (2008).
21. Abdelmoti, L. G., & Zamborini, F. P. Potential-Controlled Electrochemical Seed-Mediated Growth of Gold Nanorods Directly on Electrode Surfaces. *Langmuir.* **26** (16), 13511-13521 (2010).
22. Crick, C. R.,, *et al.* Advanced analysis of nanoparticle composites - a means toward increasing the efficiency of functional materials. *RSC Adv.* **5** (66), 53789-53795 (2015).
23. Casavell i Solvas, X., Turek, V., Prodromakis, T., & Edel, J. B. Microfluidic evaporator for on-chip sample concentration. *Lab Chip.* **12** (20), 4049-4054 (2012).
24. Casavell i Solvas, X., *et al.* Fluorescence detection methods for microfluidic droplet platforms. *J. Vis. Exp.* (58), e3437 (2011).
25. Köllner, M., *et al.* Fluorescence pattern recognition for ultrasensitive molecule identification: comparison of experimental data and theoretical approximations. *Chem. Phys. Lett.* **250** (3-4), 355-360 (1996).
26. Köllner, M., & Wolfrum, J. How many photons are necessary for fluorescence-lifetime measurements? *Chem. Phys. Lett.* **200** (1-2), 199-204 (1992).
27. Edel, J. B., Eid, J. S., & Meller, A. Accurate Single Molecule FRET Efficiency Determination for Surface Immobilized DNA Using Maximum Likelihood Calculated Lifetimes. *J. Phys. Chem., B.* **111** (11), 2986-2990 (2007).
28. Bear, J. C., *et al.* Doping Group IIB Metal Ions into Quantum Dot Shells via the One-Pot Decomposition of Metal-Dithiocarbamates. *Adv. Opt. Mater.* **3** (5), 704-712 (2015).
29. Li, L., Hu, J., Yang, W., & Alivisatos, A. P. Band Gap Variation of Size- and Shape-Controlled Colloidal CdSe Quantum Rods. *Nano Letters.* **1** (7), 349-351 (2001).

